Fracture mechanism of Al-Al_4C_3 nanomaterials studied by "in-situ tensile test in SEM"

M. Besterci[1], O. Velgosová[2]*, J. Ivan[3], P. Hvizdoš[1], T. Kvačkaj[4], P. Kulu[5]

[1] *Institute of Materials Research, Slovak Academy of Sciences, Watsonova 47, 043 53 Košice, Slovak Republic*
[2] *Department of Non-ferrous Metals and Waste Treatment, Faculty of Metallurgy, Technical University, Letná 9/A, 042 00 Košice, Slovak Republic*
[3] *Institute of Materials and Machine Mechanics, Slovak Academy of Sciences, Račianska 75, 838 12 Bratislava, Slovak Republic*
[4] *Department of Metals Forming, Faculty of Metallurgy, Technical University, Vysokoškolská 4, 042 00 Košice, Slovak Republic*
[5] *Tallinn Technical University, Department of Materials Technology, Ehitajate tee 5, 190 86 Tallinn, Estonia*

Received 4 March 2009, received in revised form 18 May 2009, accepted 18 May 2009

Abstract

The deformation and fracture mechanisms of Al-Al_4C_3 nanomaterials with 4 vol.% of Al_4C_3 phase have been analysed using technique of the "in-situ tensile testing in SEM". It has been shown that the deformation process causes break-up of large Al_4C_3 particles and decohesion of smaller ones. The final fracture path is influenced also by boundaries of nanograins, through which the principal crack propagates towards the sample exterior surface. Based on the experimental observations a model of damage and/or fracture mechanisms has been proposed.

K e y w o r d s: dispersion strengthened Al, nanomaterials, in-situ tensile testing in SEM, model of the fracture mechanism

1. Introduction

The method of "in-situ tensile testing in SEM" is suitable for investigations of fracture mechanisms because it enables to observe and document deformation processes directly, thank to which the initiation and development of plastic deformation and fracture can be reliably described.

In our previous works [1–8] and based on papers by other authors [9–11] we used "in-situ tensile test in SEM" to analyse deformation processes in various types of Cu- and Al-based composites. In works [9–11] Al-Si-Fe and Al-Si systems were studied by "in-situ tensile test in SEM". The result was a design of several models of damage, which considered physical and geometrical parameters of matrix and particles.

The dispersion strengthened alloys Al-Al_4C_3 manufactured by mechanical alloying using powder metallurgy technology are promising structural materials. One microstructured material of such type with 4 vol.% Al_4C_3 was transformed by the ECAP (Equal Channel Angular Pressing) method in two passes into a nanocomposite material. The experimental material was pressed through two right angled (90°) channels of a special die by route "C". The ECAP technology allows obtaining the very fine-grained microstructure – nanostructure by multiple pressings through the die (Fig. 1).

The aim of the work is to analyse the fracture mechanism of Al-Al_4C_3 nanocomposite system and to propose a damage model.

2. Experimental materials and methods

The starting experimental materials were prepared by mechanical alloying. Al powder of particle size of < 50 μm was dry milled in an attritor for 90 min with the addition of graphite KS 2.5 thus creating 4 vol.% of Al_4C_3. The specimens were then cold pressed us-

*Corresponding author: tel.: +421 55 602 2427; fax.: +421 55 602 2428; e-mail addresss: oksana.velgosova@tuke.sk

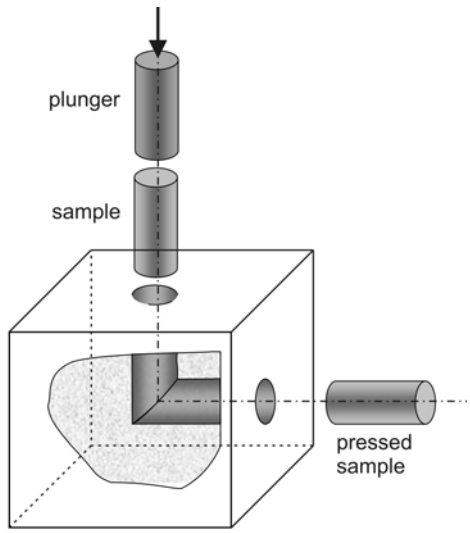

Fig. 1. Scheme of ECAP.

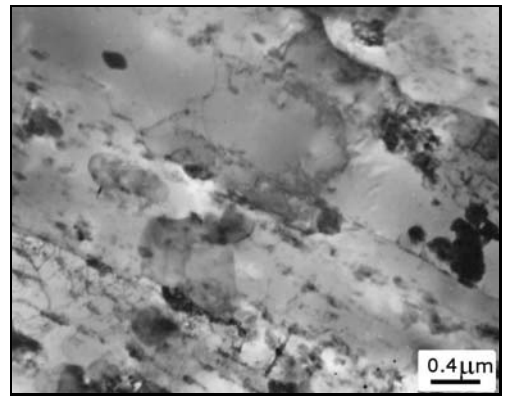

Fig. 2. Microstructure of the starting material.

ing a load of 600 MPa. The specimens had cylindrical shape. Subsequent heat treatment at 550 ℃ for 3 h induced chemical reaction $4Al + 3C \rightarrow Al_4C_3$. The cylinders were then hot extruded at 600 ℃ with 94 % reduction of the cross section. Due to a high affinity Al to O_2 the system also contains a small amount of Al_2O_3 particles. The volume fraction of starting Al_2O_3 was low, 1 vol.%. Detailed technology preparation is described in [11–14].

This material with dimensions of ø 10 × 70 mm^2 was deformed by the ECAP technique in two passes at room temperature in a hydraulic press in the equipment described in [15]. In the work [16] a dislocation model of microcrystalline system with hard nanoparticles has been suggested. Analyses of microstructure and mechanical properties evolution in ECAP are given in [17–20].

For the purposes of investigation very small flat tensile test pieces (7 × 3 mm, gauge length 7 mm) with 0.15 mm thickness were prepared by electroerosive machining, keeping the loading direction identical to the direction of extrusion. The specimens were ground and polished down to a thickness of approximately 0.1 mm. Finally, the specimens were finely polished on both sides by ion gunning. The test pieces were fitted into special deformation grips inside the scanning electron microscope JEM 100 C, which enabled direct observation and measurement of the deformation by ASID-4D equipment. From each one of the systems five samples were prepared.

3. Results and discussion

The microstructure of the starting material with 4 vol.% Al_4C_3 was fine-grained (the mean matrix grain size was 0.35 μm), heterogeneous, with Al_4C_3 particles distributed in parallel rows as a consequence of extrusion. Beside the phase Al_4C_3, the systems contained also Al_2O_3 phase (∼ 1 vol.%). Essentially, it was the remnant of oxide shells of the original matrix powder and/or shells formed during the reaction milling in attritors.

When describing microstructures, one has to consider geometrical and morphological factors. According to the microstructure observations, the particles in our materials can be divided into three distinctive groups: A – small Al_4C_3 particles, identified by TEM, with mean size approximately 30 nm which made up to 70 % of the dispersoid volume fraction; B – large Al_4C_3 particles with mean size between 1 and 2 μm, identified by scanning electron microscopy and on metallographic micrographs; and C – large Al_2O_3 particles with mean size of 1 μm, found on metallographic micrographs and identified by scanning electron microscopy. Morphologically, Al_4C_3 particles are elongated and Al_2O_3 particles are spherical. Let us assume that particles of all categories during the high plastic deformation are distributed in rows. Mean distance between the rows is l and between the particles h. The particles are spherical or have only a low aspect ratio, so that they can be approximated as spherical ones. The experimental materials were deformed at 20 ℃ at a strain rate of 6.6×10^{-4} s^{-1} in the elastic region.

The material after ECAP is on the border of nanostructured materials. The TEM micrographs, Fig. 2 and Figs. 3a,b showed that the mean grain size was 100–200 nm, dislocations are present in nanograins, too, but mostly on the boundaries. In Fig. 3 are these dislocations weakly visible due to the tilting of the specimen. The nanostructure formation takes place most probably by a three-stage mechanism, described in [20]. This model has been experimentally verified only for several specific materials but in our case it seems to be probably usable. The model includes cre-

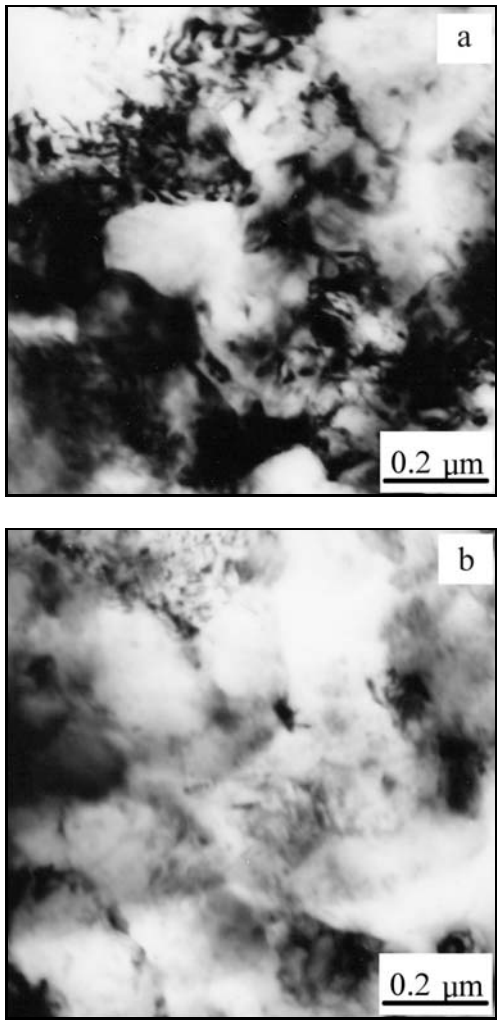

Fig. 3. Microstructures of the material after ECAP.

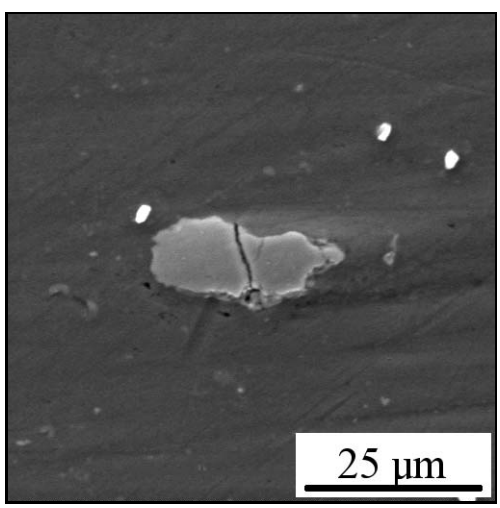

Fig. 4. Fracture of B-type, particles Al_4C_3 in the middle of the layer.

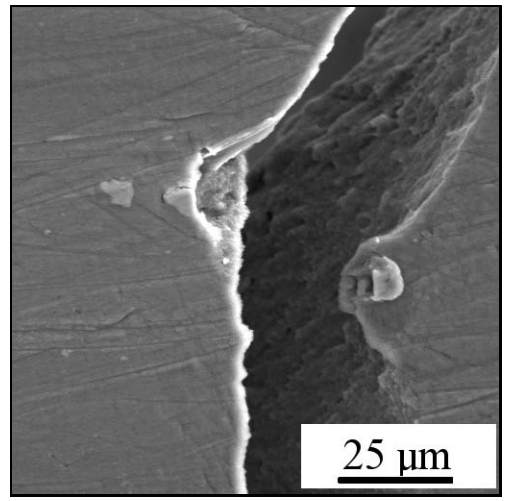

Fig. 5. Final fracture of large particles.

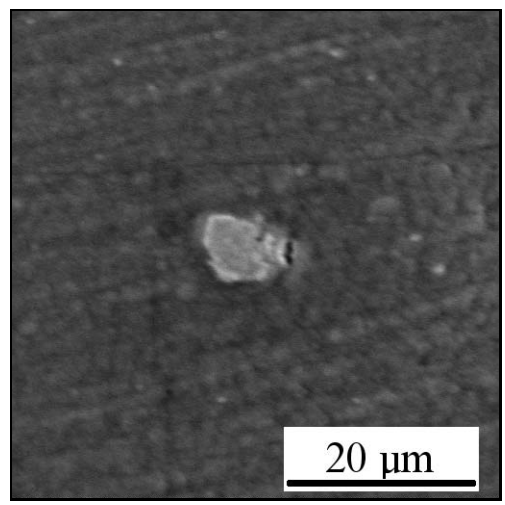

Fig. 6. Decohesion of smaller particles, C-type Al_2O_3.

ation of cell structure, then formation of transitory cell nanostructure with large angle disorientation, and finally formation of nanostructured grains with size of approx. 100 nm. However, here one has to consider the retarding effect due to present dispersoid particles.

Deformation process of the loaded layer causes fracture of large, B-type, particles in the middle of the specimen (Figs. 4 and 5), which initializes fracture path roughly perpendicular to the loading direction (Fig. 6). The fracture path is determined also by decohesion of smaller particles (type A and/or C). Since the volume fractions of Al_4C_3 and Al_2O_3 particles are small, their distribution in lines does not influence the trajectory of fracture which has low relative deformation $\varepsilon = 0.135$. Unlike the microstructured Al-based composites, in this case it has been shown that the nanograin boundaries play an important role. In

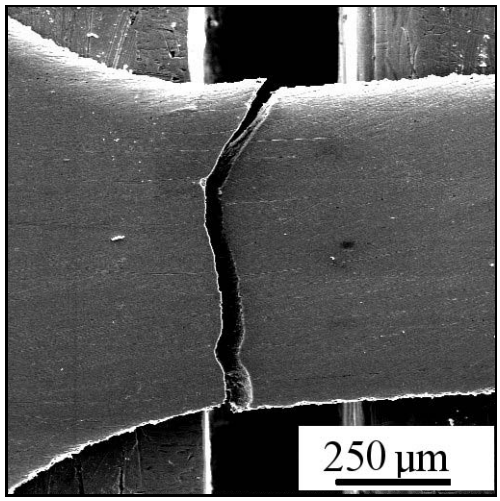

Fig. 7. The final phase of the crack.

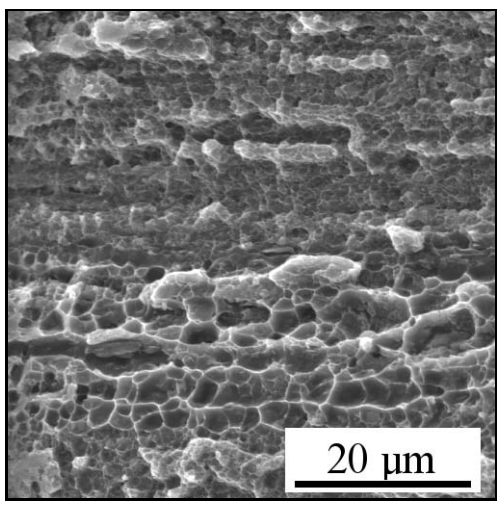

Fig. 8. Surface morphology of the material with 12 vol.% Al_4C_3.

the final phase (Fig. 7) a crack propagates along the nanograin boundaries, which has been observed experimentally on the crack line (profile), and it is documented also by the ductile fracture surface with typical dimples in Fig. 8.

A detailed study of the deformation changes showed that the crack initiation was caused by decohesion, and occasionally also by rupture of the large particles. Decohesion is a result of different physical properties of different phases of the system. The Al matrix has significantly higher thermal expansion coefficient and lower elastic modulus (from 23.5 to 26.5 $\times$ 10^{-6} K^{-1}, and 70 GPa) than both Al_4C_3 (5 $\times$ 10^{-6} K^{-1}, and 445 GPa) and Al_2O_3 (8.3 $\times$ 10^{-6} K^{-1}, and 393 GPa), respectively. Large differences in the thermal expansion coefficients result in high stress gradients, which arise on the interphase boundaries during the hot extrusion. Since $\alpha_{\mathrm{matrix}} > \alpha_{\mathrm{particle}}$, high compressive stresses can be expected. However, because the stress gradients arise due to the temperature changes, during cooling (which results in increase of the stress peaks) their partial relaxation can occur. Superposition of the external load and the internal stresses can initiate cracking at interphase boundaries. This is in accordance also with the dislocation theories which argue that the particles in composite may cause an increase in the dislocation density as a result of thermal strain mismatch between the ceramic particles and the matrix during preparation and/or thermal treatment [16]. In our case, the coefficient of thermal expansion of the matrix is much higher than that of the secondary particles and the resulting thermal tension may relax around the matrix-particle interfaces by emitting dislocations, whose density can be calculated according to procedure described in [16].

Based on the microstructure changes observed in the process of deformation, the following model (it is not a general model but one that resulted from our experiments) of fracture mechanism is proposed (Fig. 9a,b,c,d):

a) The microstructure in the initial state is characterized by Al_4C_3 and Al_2O_3 particles, categorized as A, B and C, whose geometric parameters (l, h and d) depend on their volume fraction.

b) With increasing tensile load, local cracks, predominantly on specimen side surfaces, are formed by rupture of large (B) and decohesion of smaller (C and/or A) particles.

c) In further increasing deformation of nanocomposite materials the nanograin boundaries start to play an important role. Since the volume fraction of these boundaries is high and the size of the B and C particles is equal to the matrix grain size, crack propagates preferentially along the nanograin boundaries.

4. Conclusion

The aim of the study was to evaluate the influence of volume fraction of Al_4C_3 (4 vol.%) and Al_2O_3 (1 vol.%) particles on the fracture mechanism by means of the method "in situ tensile test in SEM".

Based on the microstructure changes obtained in the process of deformation of the dispersion strengthened Al-Al_4C_3 alloys, a model of fracture mechanism was proposed. With increasing tensile load the local cracks, predominantly on specimen's side surfaces, are formed by rupture of large (B) and decohesion of smaller (C, A) particles. The orientation of cracks tends to be perpendicular to the loading direction, depending on the particle volume fraction. The final rupture, i.e. interconnection of the side

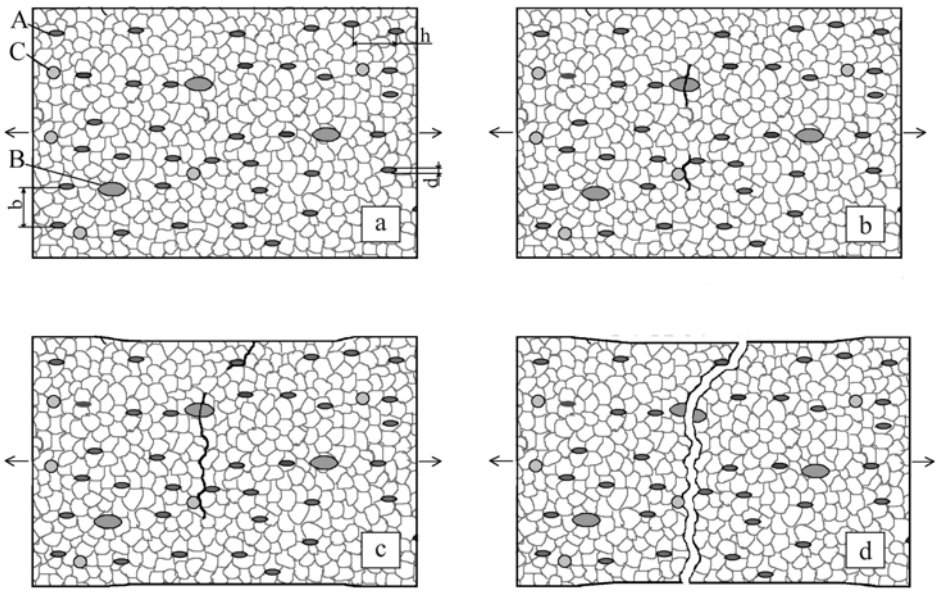

Fig. 9a,b,c,d. Model of the fracture mechanism.

cracks along the loading direction, takes place at nanograin boundaries, depending on the volume fractions of carbide (Al_4C_3) and oxide (Al_2O_3) particles.

Acknowledgements

The work was supported by the Slovak National Grant Agency under the Project VEGA 2/0105/08.

References

[1] BESTERCI, M.—IVAN, J.: J. of Mater. Sci. Lett., *15*, 1996, p. 2071.
[2] BESTERCI, M.—IVAN, J.: J. of Mater. Sci. Lett., *17*, 1998, p. 773.
[3] BESTERCI, M.—IVAN, J.—KOVÁČ, L.—WEISS-GAERBER, T.—SAUER, C.: Mat. Letters, *38*, 1999, p. 270.
[4] BESTERCI, M.—IVAN, J.—KOVÁČ, L.—WEISS-GAERBER, T.—SAUER, C.: Kovove Mater., *36*, 1998, p. 239.
[5] BESTERCI, M.—IVAN, J.—KOVÁČ, L.: Kovove Mater., *38*, 2000, p. 21.
[6] BESTERCI, M.—IVAN, J.—KOVÁČ, L.: Materials Letters, *46*, 2000, p. 181.
[7] BESTERCI, M.—IVAN, J.—VELGOSOVÁ, O.—PEŠEK, L.: Kovove Mater., *39*, 2001, p. 361.
[8] BESTERCI, M.—VELGOSOVÁ, O.—IVAN, I.—HVIZDOŠ, P.—KOHÚTEK, I.: Kovove Mater., *46*, 2008, p. 139.
[9] MOCELLIN, A.—FOUGEREST, F.—GOBIN, P. F. J.: Mater. Sci., *28*, 1993, p. 4855.
[10] VELÍSEK, R.—IVAN, J.: Kovove Mater., *32*, 1994, p. 531.
[11] BROUTMAN, L. V.—KROCK, R. H.: Compos. Mater., *5*, 1974, p. 27.
[12] JANGG, G.—VASGURA, H.—SCHRÖDER, K.—ŠLESÁR, M.—BESTERCI, M.: In: Int. Conf. Powder Metallurgy (PM 86). Eds.: Kaysser, W. A., Huppmann, W. J. Freiburg, Verlag Schmid GmbH 1986, p. 989.
[13] KORB, G. —JANGG, G.—KUTNER, F.: Draht, *30*, 1979, p. 318.
[14] ŠALUNOV, J.—ŠLESÁR, M.—BESTERCI, M.—OPPENHEIM, H.— JANGG, G.: Metall, *6*, 1986, p. 601.
[15] BESTERCI, M.—SÜLLEIOVÁ, K.—KVAČKAJ, T.: Kovove Mater., *46*, 2008, p. 309.
[16] LUKÁČ, P.—TROJANOVÁ, Z.: Kovove Mater., *44*, 2006, p. 243.
[17] VALIEV, R. Z.: Nanostructured Materials, *6*, 1995, p. 73.
[18] VALIEV, R. Z.: In: Proceedings of Metallic Materials with High Structural Efficiency. NATO Science Series, Kijev. Eds.: Senkov, O. N., Miracle, D. B., Firstov, S. A. Amsterdam, IOS Press and Dordrecht, Kluwer Acad. Publishers 2003, p. 79.
[19] ZHU, Y. T. et al.: J. Mater. Res., *18*, 2002, p. 1908.
[20] VALIEV, R. Z.—ALEXANDROV, I. V.: Nanostrukturnyje materialy polučennyje intensivnoj plastičeskoj deformaciej. Moskva, Logos 2000.